ELSEVIER

International Journal of Mass Spectrometry 182/183 (1999) 357–368

International Journal of Mass Spectrometry

Investigation of dialkyl tartrate molecular recognition in cluster ions by Fourier transform mass spectrometry: a comparison of chirality effects in gas and liquid phases

E.N. Nikolaev[1], E.V. Denisov[1], V. Sergey Rakov, Jean H. Futrell*

University of Delaware, Newark, DE 19716, USA

Received 5 August 1998; accepted 4 November 1998

Abstract

Electrospray ionization of equimolar solutions of *S*-dimethyl tartrate and *R*-*d*6-dimethyl tartrate in methanol/water/acetic acid/salt solutions was utilized to investigate molecular recognition processes in solution. Pronounced chirality effects previously reported for formation of the protonated dimer by ion molecule reactions in the gas phase are quantitatively reproduced in experiments which sample solution phase protonated dimers. Ab initio quantum calculations demonstrate that hydrogen bonds in the protonated cluster are responsible for molecular recognition and that Li^+ bound clusters, which do not exhibit chiral recognition, are primarily bound by electrostatic forces. In contrast with gas phase studies of alkali and ammonium ion core dimers of dimethyl tartrate—which show no chirality effects—ions electrosprayed from solutions containing trace amounts of these ions show pronounced chirality. With increasing salt concentration the apparent chirality effect disappears and a statistical distribution identical to that found for the gas phase is obtained. These observations are rationalized by a kinetic model that considers the displacement of protons by alkali ions in the final stages of desolvation of microdroplets formed in the electrospray process. (Int J Mass Spectrom 182/183 (1999) 357–368) © 1999 Elsevier Science B.V.

Keywords: Dialkyl tartrate molecular recognition; Cluster ions; FTMS; Chirality; Gas and liquid phases

1. Introduction

This article is a progress report on our continuing investigation by Fourier transform mass spectrometry (FTMS) of chirality effects in ion clusters of alkyl tartrate molecules. The general topic of mass spectrometry studies of chiral recognition has recently been reviewed by Sawada et al. [1] and studies specifically of dialkyl tartrates have been reviewed by us [2]. This class of model compounds has a number of advantages for investigating molecular recognition quantitatively. Their vapor pressures are high enough for gas phase studies by mass spectrometry, standards of known chirality are readily available and they are small enough to model with high level quantum chemistry methods. The first report of chiral preference in ion clusters of these molecules was a high pressure chemical ionization mass spectrometry study

* Corresponding author.

[1]Permanent address: Institute for Energy Problems of Chemical Physics Russian Academy of Sciences, Moscow, Russia.

Dedicated to the memory of Ben Freiser to commemorate his many seminal contributions to mass spectrometry and gas phase ion chemistry.

PII S1387-3806(98)14275-6

by Fales and Wright on protonated dimethyl tartrate and di-isopropyl tartrate dimers [3]. About a decade later we and others extended these studies to address relative stabilities and formation/decomposition ion kinetics. We have previously reported on our studies of formation and decomposition kinetics of dialkyl tartrates clusters in the gas phase at various temperatures and with different core ions [2,4]. It was found that both the sign and magnitude of the chirality effect vary with the core ion and the number of molecules in the cluster [2]. Quantum chemistry calculations presented earlier in preliminary form [2] and summarized below demonstrate that molecular recognition in protonated clusters is communicated by formation of hydrogen bonds. We previously attempted—with limited success—to investigate the effect of solvation (by water molecules) on the stability of chiral molecule clusters [2,5]. In the present paper we extend this to the limit of full solvation, using electrospray ionization to sample the chiral distribution of cluster ions extracted from solution. A strong chirality effect on dimer and trimer formation was observed for alkali and ammonium clusters which do not exhibit chirality in gas phase experiments. Although the complicated mechanism(s) of ion formation in electrospray ionization (ESI) precludes a comprehensive explanation for the origin of chiral effects observed in ESI spectra, we present here a simplified kinetics scheme which satisfactorily rationalizes our observations. The starting point of our analysis is that the distribution of enantiomeric alkali ion dimers is fixed by decomposition of unstable trimers formed in the final stage of desolvation of microdroplets in the electrospray process.

2. Experimental methods

Chirality effects were determined by comparing the mass-spectral intensity ratios of *SS*:*RS*:*RR* dimer and *SSS*:*SSR*:*SRR*:*RRR* trimer ions for nearly equimolar mixtures of unlabeled *S*-dimethyl tartrate (*S*-DMT) and *R*-*d*6-dimethyl tartrate (*R*-DMT) in gas phase chemical ionization (CI) conditions and in solution as sampled by electrospray ionization. Labeled tartrates were synthesized by substitution of *D* for *H* in methyl groups of unlabeled tartrates by potassium salt catalyzed exchange with deuterated methyl alcohol. In one series of experiments we utilized an analogous mixture of unlabeled and labeled di-isopropyl tartrates.

Gas phase results were obtained using a Finnigan FTMS 2000 instrument fitted with an external ion source of our own design shown schematically in Fig. 1. A chemical ionization source of our own design was used to generate protonated cluster ions. In other experiments a CO_2 laser was used to ablate alkali metal ions from the tip of the solids insertion probe into the ion cyclotron resonance (ICR) cell for forming alkali ion core clusters in the gas phase. Simultaneously the probe was gently heated to establish an (uncorrected) ion gauge pressure reading of 5–10 $\times$ 10^{-6} Torr of the dimethyl tartrate mixture in the ICR cell to form alkali ions—tartrate cluster ions.

Solution chirality effects were investigated using a Bruker Daltonics BioApex 7T shielded magnet FTMS fitted with an Analytica electrospray ion source. Water-methanol-acetic acid mixtures of deuterium-labeled *R*-DMT and unlabeled *S*-DMT containing trace quantities of Li^+, Na^+, and K^+ were electrosprayed and resulting ions were injected into the ICR cell and trapped for mass analysis. Different concentrations of alkali metal ions were then deliberately added to solutions to evaluate dependence of chirality on composition. Electrospray conditions were varied over normal working ranges to evaluate effects of varying voltages on the skimmer, lenses and the hexapole section. Metal and glass capillaries were used in different experiments at two different temperatures.

Theoretical calculations utilized MM+ molecular dynamics simulations of the dimer structures using Hyperchem program to obtain trial conformations which were then optimized using the B3P86 density functional in the 3-21G** basis set in GAUSSIAN-94[6] program. Starting geometries for *SR* and *RR* DMT dimers coordinated on proton and Li^+ ion, respectively, were first obtained by a force field approximation optimization. These structures were annealed by the force field molecular dynamics to generate 50 geometries for each dimer in the region of converged

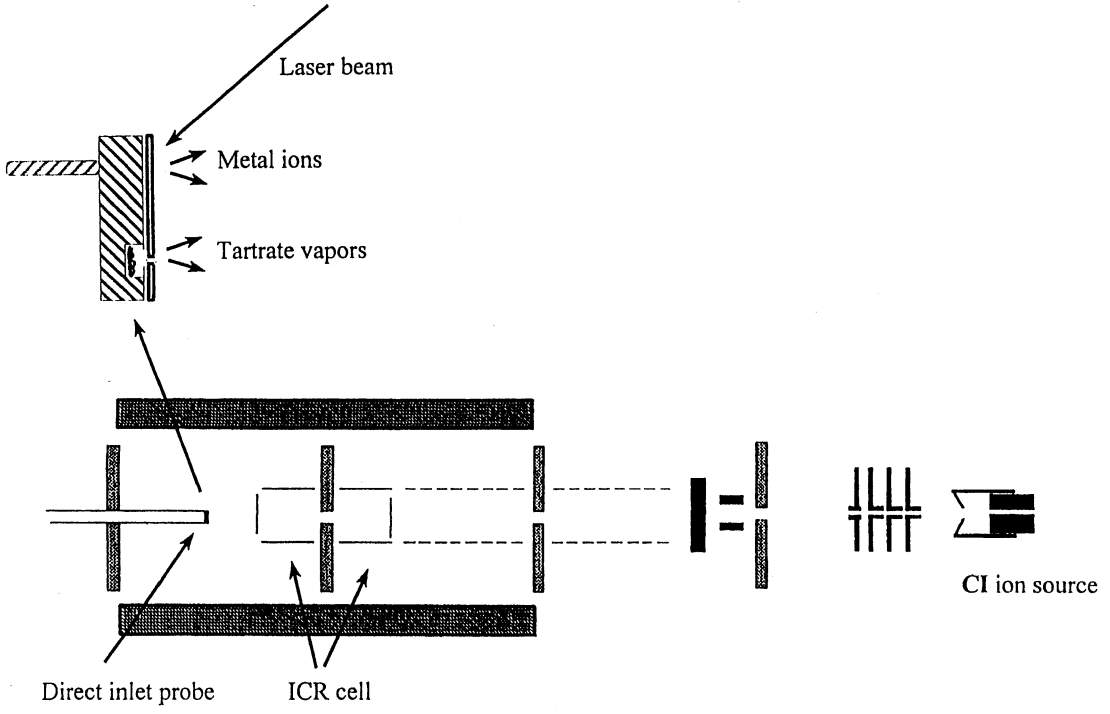

Fig. 1. Finnigan FTICR mass spectrometer showing external ionization CI source and modified direct inlet probe nonvolatile sample holder. In *A* cavity was drilled into the removable probe tip for DMT samples and a foil with a pinhole covering the cavity on which salt solutions were evaporated from dilute aqueous solutions was attached as a source of alkali ions during laser ablation. The CI source was used to study ion equilibrium in protonated DMT clusters and a laser ablation source was used to investigate DMT cluster formation in FTICR cell by reaction of ablated metal ions with DMT vapors evaporated from the cavity.

lowest energy. Median energy structures were then optimized by the density functional theory (DFT[7]) method in GAUSSIAN94. These lowest energy states were used to compare stabilities of *SR* and *RR* protonated and lithium cation dimers.

3. Results and discussion

3.1. Gas phase results and theoretical modeling

We have previously reported strong chirality effects observed when an approximately equimolar mixture of *S*-*d*6-dimethyl tartrate and *R*-*d*6-dimethyl tartrate is ionized in a chemical ionization source using the Fig. 1 apparatus. Protonated dimers, trimers and tetramers exhibit very strong chirality effects, with intensity ratios of approximately 1:0.5:1, 1:5:5:1, and 1:3:4:3:1 (adjusted for an equimolar *S*-DMT/*R*-*d*6-DMT mixture) rather then the statistically-predicted 1:2:1, 1:3:3:1, and 1:4:6:4:1, respectively. Interestingly, the distribution switches from favoring the homochiral distribution at the dimer stage to enhanced heterochiral structures for the trimer. In the present paper we focus our attention on the dimer structure, on the effect of changing the core ion to alkali cations and on a comparison of electrosprayed ion distributions with those obtained in the gas phase.

Fig. 2 shows the distribution in the dimer group obtained by reacting Li^+ cations with the same dimethyl tartrate mixture. This spectrum was generated using the Fig. 1 apparatus with laser desorption of Li^+ from trace amounts of LiCl deposited on the probe tip. Dimethyl tartrate is sufficiently volatile to give a background pressure of the order of 10^{-5} Torr in the ICR cell when the probe is warmed gently. Li^+

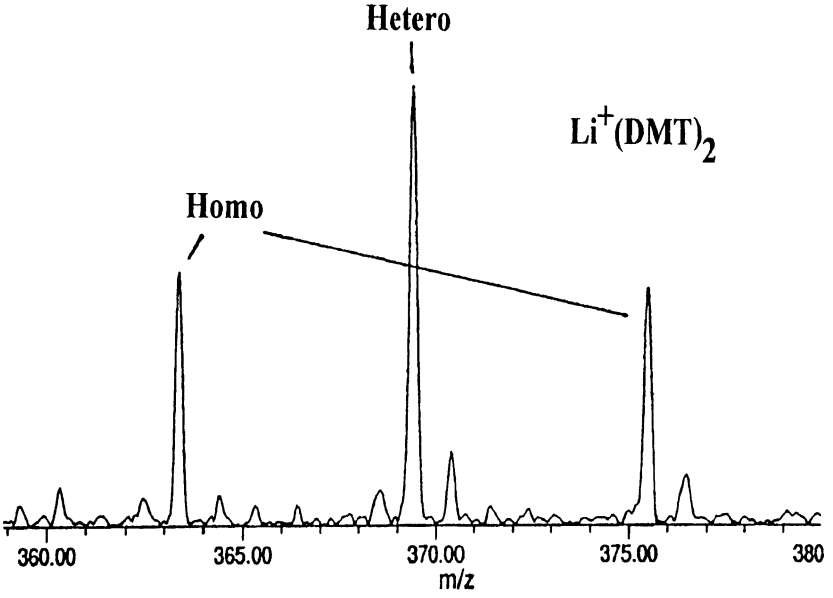

Fig. 2. FTICR spectrum of LI^+ based DMT dimers, generated by reaction of laser ablated Li^+ ions with DMT vapors in the Fig. 1 apparatus.

ions generated by laser evaporation react with dimethyl tartrates. Following a sequence of ion molecule and ligand exchange reactions the Fig. 2 spectrum is formed. In sharp contrast with protonated dimethyl tartrate, the distribution matches very well the statistically-predicted ratio of 1:2:1. Similar results were obtained with Na^+, K^+, and Cs^+ core ions, demonstrating the absence of molecular recognition leading to chirality effects in alkali cation dimers [2].

The relative stability of heterochiral and homochiral alkali cation dimers was explored experimentally by collisional activation of translationally excited dimers. Carbon dioxide was used as the collision gas. We found the collision-activated dissociation (CAD) rates to be identical for all chiral structures. That is, both homochiral and heterochiral dimers decay synchronously, consistent with the hypothesis that the dimer is bound by mainly long-range forces which do not distinguish enantiomeric structures.

The probable cause for pronounced chirality in protonated dimers and absence of chirality in alkali ion core dimers was established by quantum chemical modeling simulations of the respective dimer ion structures. We utilized force field molecular dynamics (with annealing) to generate trial structures of proton-bound and alkali-metal-ion bound *SS* and *SR* DMT dimers. An ensemble of 50 randomized structures in the region of converged total force-field energy provided us with a distribution of geometries (and corresponding total energies) under relatively crude approximations employed by MM+ force-field calculations. We then selected four "typical structures" from the low energy group of structures; the standard deviation of the mean energy did not exceed 8% for any of the four dimer ensembles investigated.

The selected four "typical" structures, one for each dimer, which were then optimized more rigorously using the B3P86 density functional method in the 3-21G** basis set of the GAUSSIAN-94 program. This choice is a reasonable compromise between computational costs and experimental precision. Ground state DFT-corrected energies [E(RB + HF − VWN − P86)] (where RB, HF, VWN, and P86 stand for Restricted Becke; Hartree-Fock; Vosko-Wiek-Nusair; and Perdew-86 functionals and correlation functionals, respectively [7]) for Li^+ bound *RR* and *SR* dimers, thus generated, differed by 2.5 kcal/mol, which is only a few times *kT*. For the proton bound dimers the *RR* structure was more stable than *SR* by 7 kcal/mol. Energy of formation of *SR* Li^+ bound *SR*

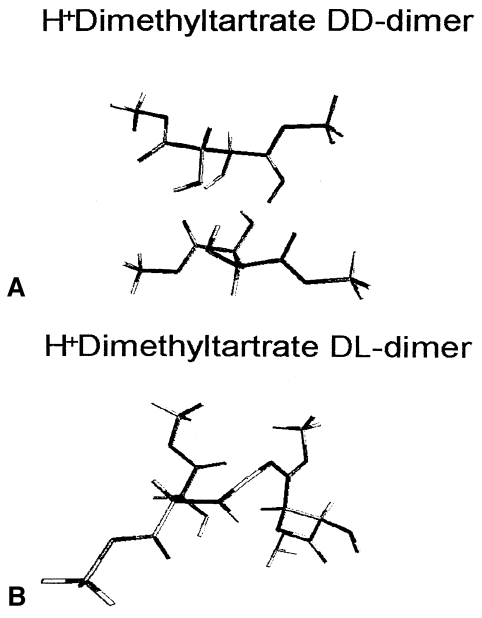

Fig. 3. Optimized structures of protonated (a) homo- and (b) hetero-DMT dimers. B3P86 functional optimization with 3-21G** basis set.

dimer was estimated by comparing the total DFT corrected energy obtained in this calculation to the total energy of optimized structures of dissociation products, Li^+—DMT adduct and DMT monomer. The binding energy was 69 kcal/mol (~3 eV) representing a theoretical upper bound to its dissociation energy. The analogous comparison for proton bound dimer dissociation gives an upper bound dissociation energy of 53 kcal/mol.

Figs. 3(a) and 3(b) show representative optimized B3P86/3-21G** structures for the homochiral and heterochiral protonated dimers, respectively. It is noteworthy that the proton bridge is best described as a hydrogen bond with the charge widely distributed over the structure rather than localized at the proton. Detailed analysis of interatomic distances in the 3D structure demonstrates that the Fig. 3(a) structure contains six hydrogen bonds, whereas the Fig. 3(b) structure contains only five. The Fig. 3(a) structure is 7 kcal/mol lower in DFT corrected ground state energy than the Fig. 3(b) structure. This energy/structural difference rationalizes the experimental preference in the dimer cluster for homochiral structures.

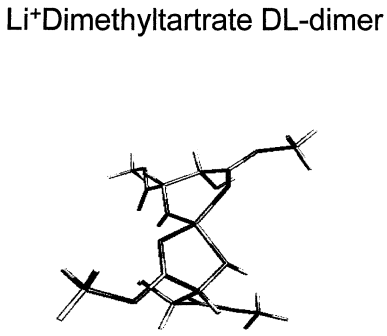

Fig. 4. Optimized structure of Li^+ based homochiral DMT dimers using the B3P86 functional optimization in the 3-21G** basis set.

As noted, this analysis of bonding and relative bond strengths in heterochiral versus homochiral structures is consistent with our experimental studies of alkyl tartrate cluster equilibria and kinetics in the gas phase. We have demonstrated that the rates of formation of both types of dimers are identical, with ion-neutral collision cross-sections characteristically dominated by long range forces [2]. The preference for homochiral structures in the relaxed dimer results from the relatively higher unimolecular dissociation rate of the heterochiral dimer. The higher zero point energy of the heterochiral structure and relatively shallow potential well for proton-bound dimers are in good agreement with reaction rates and thermochemistry previously reported for this system [2].

Fig. 4 shows a typical optimized B3P86/3-21G** structure for the lithium cation dimer calculated in the manner just described. For this example the cluster ion structure is distinctly different from the Fig. 3 structures. In particular, for this cluster the charge remains localized on the Li nucleus and there is no more than one hydrogen bond between the tartrate moieties. The core ion coordinates the DMT monomers in almost exact orthogonal cross geometry expected for predominantly ionic bonding. For this dimer the core ion does not allow the monomers to come close enough to each other to exhibit chiral recognition. Because the mechanism for molecular recognition found in the protonated analog is absent here, this model predicts that no chiral effect should be observed consistent with our experimental results.

A final point concerns the relative stability of

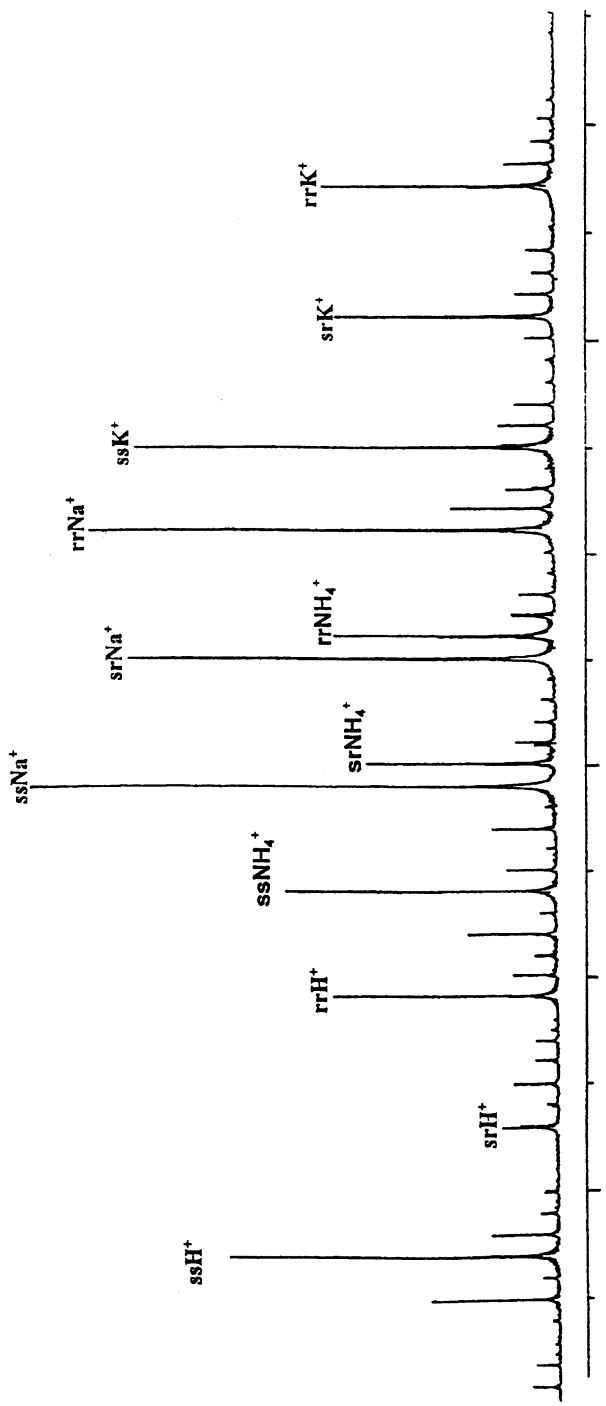

Fig. 5. FTICR spectrum of Na^+, K^+, NH_4^+, and H^+ based DMT dimers produced by ESI from 300 μM concentration DMT solution in 50:50:1 water:methanol:acetic acid mixture containing traces of alkali and ammonium ions.

protonated dimers and alkali ion dimers. The theoretical calculations, just described, indicate that the Fig. 4 lithium ion adduct is more stable than the Fig. 3(a) structure by about 16 kcal/mol, with an uncertainty of the order of 8 kcal/mol. It is not expected that our calculations at this level of accuracy can reliably predict the relative stability of these two types of clusters. However, the theoretical result is strongly supported by ion trapping measurements which confirm the higher stability of alkali cation clusters. For example, the isolation of K^+ core alkali ion dimers for periods of 100 s gave no evidence for their decomposition into adduct ions and monomers. In contrast, proton-bound dimers dissociate in storage times of this duration. Specifically, heterochiral dimers have a lifetime at room temperature of about 10 s and homochiral dimers, about 100 s [8].

3.2. Solution phase clusters

Fig. 5 illustrates dimer cluster distributions obtained from electrospray ionization sampling of a 300 micromolar solution of an equimolar mixture of *S*- and *R*-*d*6-dimethyl tartrates electrosprayed from a methanol/water/acetic acid solution containing trace amounts of sodium, potassium and ammonium ions. The spectrum demonstrates a strong chirality effect with the distribution of approximately 1:0.1:0.8 rather then the statistical 1:2:1. The chirality effect is slightly stronger than that obtained in the gas phase under equilibrium conditions [2]. This can be rationalized if electrosprayed ions have a slightly lower temperature after they are expanded from a capillary and desolvated than ions generated by room temperature chemical ionization reactions. We infer from the very similar chirality effect that solvation in the liquid phase does not disturb substantially the hydrogen bonded structure found for relaxed ions in the gas phase and calculated theoretically in Fig. 3. This is a surprising result because our previous study of gas phase clusters showed that the addition of one molecule of water to a protonated cluster reverses the chirality effect at the dimer and trimer stages [2]. The substitution of H_3O^+ as a core ion for the hydrogen bonded Fig. 3 cluster evidently results in a very different H-bonded structure which strongly favors the heterochiral dimer. Further, there is no evidence in Fig. 5 that hydronium core dimers are formed and we may infer that ligand switching—e.g. from H^+ to H_3O^+—observed in gas phase studies does not occur in dilute aqueous solutions.

Dimers with NH_4^+, Na^+, and K^+ core ions are readily observed in Fig. 5 spectrum even though these ions are adventitiously present in only trace amounts. These dimers are all characterized by distinctly stronger chirality effect than in the statistically distributed gas phase Li^+ dimers shown in Fig. 2. The ammonium dimer distribution, which shows the same strong chirality effects in solution and no chirality (e.g. statistical distribution) in gas phase, was not investigated further. We presume that it would exhibit the same phenomenological dependence as alkali cation dimers.

As we reported previously [2], the apparent chirality effect in alkali dimers electrosprayed from methanol/water/acetic acid solutions disappears when the salt concentration approaches the tartrate ion concentration. That is, at higher salt concentration the distribution is statistical, identical to that found in our gas phase experiments. Figs. 6(a) and 6(b) report a systematic study of the dependence of the apparent chirality effect on concentration of NaCl and CsCl, respectively, in the electrosprayed solution. In these experiments the concentration of tartrate was held constant at about 1 mmol/L and the solution was 1:1:1% for water/methanol/acetic acid, identical to our previous studies [2]. [Di-isopropyl tartrate mixtures were used in this study. A less extensive DMT study gave qualitatively similar results.] Both curves exhibit the “S curve” shape in a semi-log plot which is characteristic of a phenomenon that saturates with concentration. Evidently electrosprayed ions are preformed with the same structure as in the gas phase when sodium or cesium cation concentrations in the bulk solution are greater than the concentration of dimethyl tartrate. The flattening of the sodium ion curve at low added salt levels with a higher apparent chirality coefficient than the cesium curve reflects, at least in part, the ubiquitous presence of trace quantities of NaCl in laboratory apparatus.

Ion trapping and collisional activation experiments for electrosprayed alkali cation dimers exhibit the same kinetics as gas phase dimers, as expected if structures of these ions are identical once they are trapped in the ICR cell. It is plausible that the different distributions and their variation with salt concentration results from their mechanism of formation in the electrospray process rather than from intrinsically different properties of solution phase dimers. We have previously suggested that this may result from the exchange of alkali cations for protons in protonated dimers to form the more stable alkali ion adduct in the last stage of ion formation [2]. This concept is modified and elaborated below to provide a quantitative explanation for the Fig. 6 results.

Fig. 7 conceptualizes our proposed mechanism for the Fig. 6 chirality effect in cartoons depicting two microdroplets representing two competing pathways leading to alkali-dimer formation. Both pathways postulate the transient formation of alkali trimers in the last stage of desolvation. The droplet on the left contains a protonated dimer formed with strong chiral recognition and characterized by a nonstatistical normalized distribution:

$$\frac{(1-\alpha)}{2}:\alpha:\frac{(1-\alpha)}{2} \tag{1}$$

The chiral recognition coefficient α has possible value ranging from 0–1, with zero corresponding to defining only homochiral clusters and one only heterochiral. It is conceptualized that the same droplet contains a Na^+ DMT adduct. The alkali cation adduct present in a microdroplet is *S*-DMT or *R*-DMT with equal probability for an equimolar solution. Because of the greater stability of the alkali cation dimer the alkali cation displaces the proton in the transient trimer. The transient trimer has the *SSS*:*SSR*:*SRR*:*RRR* distribution of:

$$\frac{1}{4}[(1-\alpha):(1+\alpha):(1+\alpha):(1-\alpha)] \tag{2}$$

Provided that stability of the transient intermediate trimer complex does not depend on chirality the resulting *SS*:*SR*:*RR* distribution in alkali-bound dimers resulting from the decomposition of a trimer with the Eq. (2) distribution is

$$\frac{1}{12}\{[3(1-\alpha)+(1+\alpha)]:4(1+\alpha):[3(1-\alpha)+(1+\alpha)]\} \tag{3}$$

An important deduction is that in the limit of low α, the alkali-dimer distribution approaches 1:1:1 rather than the statistical limit 1:2:1 for preformed alkali dimers.

A more rigorous model includes the possibility that heterochiral trimers may be less stable than homochiral ones. If we assign one and β to the decomposition rates for homochiral and heterochiral trimers, respectively, the final equation for the left droplet channel (1) normalized distribution becomes:

$$\frac{1}{6[(1-\alpha)+\beta(1+\alpha)]}\times[3(1-\alpha) + \beta(1+\alpha):4\beta(1+\alpha):3(1-\alpha)+\beta(1+\alpha)] \tag{4}$$

Applying analogous reasoning to the right side droplet pathway, the liquid phase alkali-bound dimer is characterized by the normalized statistical distribution of

$$\frac{1}{4}(1:2:1) \tag{5}$$

which reacts with an alkali-bound monomer distributed as 1:1, to obtain

$$\frac{1}{8}(1:3:3:1) \tag{6}$$

for the normalized distribution of the transient trimers intermediate. Including the $1:\beta$ decomposition branching ratio leads the normalized distribution

$$\frac{1}{2+6\beta}[(1+\beta):4\beta:(1+\beta)] \tag{7}$$

of *SS*:*SR*:*RR* for the right droplet channel alkali-bound dimers originating from the right droplet channel (2).

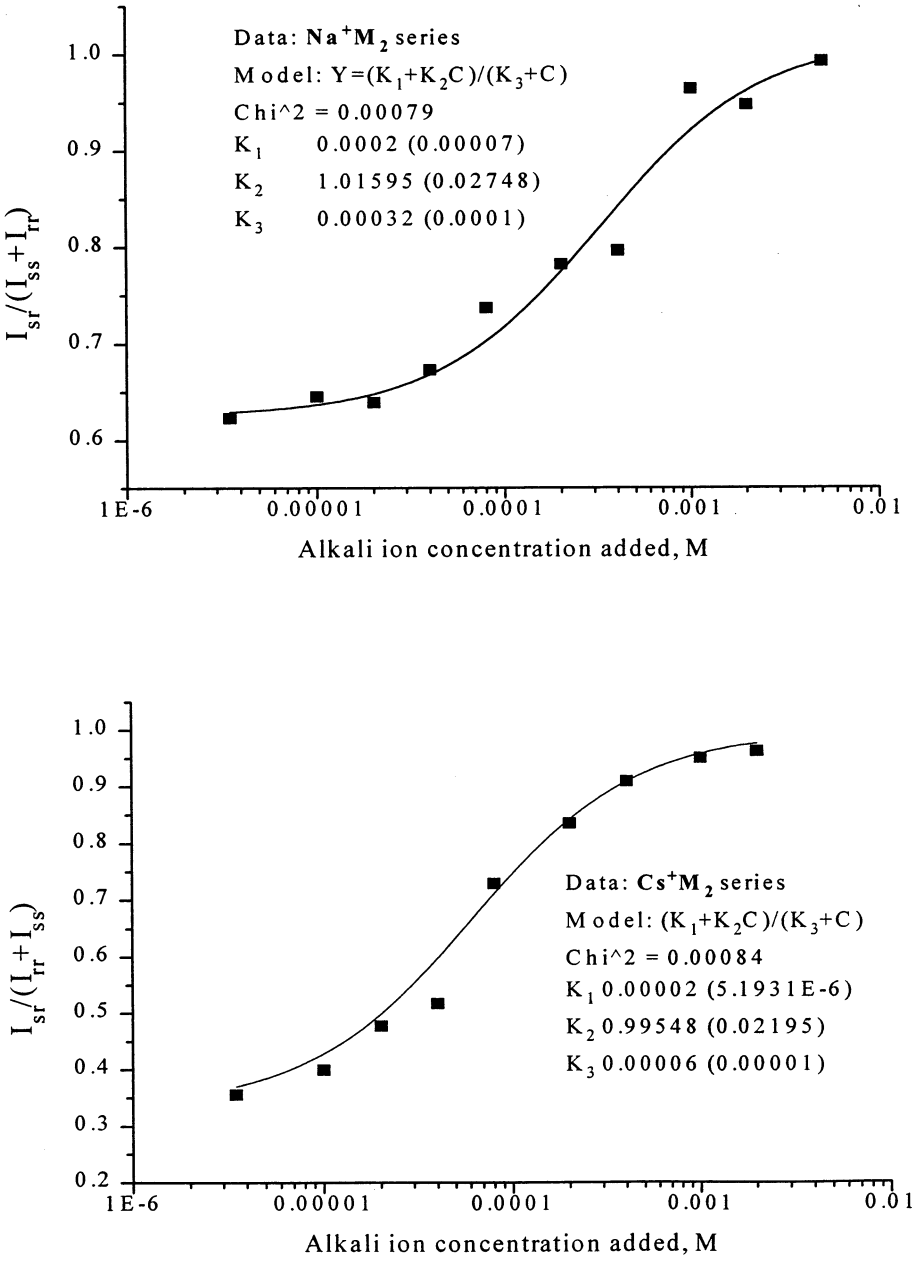

Fig. 6. Experimental dependencies of chirality effects in (a) Na^+ and (b) Cs^+ based dimers obtained by ESI from 300 μM concentration di-isopropyltartrate solution in (50:50:1) water:methanol:acetic acid mixture as a function of concentration of alkali ions.

With increasing alkali-ion concentration this second channel gradually shifts the final dimer distribution toward statistical ratios. Thus, our Fig. 7 transient trimer adduct model qualitatively rationalizes the features of the Figs. 6(a) and 6(b) dependencies of chirality on bulk concentration of alkali ions, and also accounts for the low salt concentration asymptote not equaling the proton bound dimer limit.

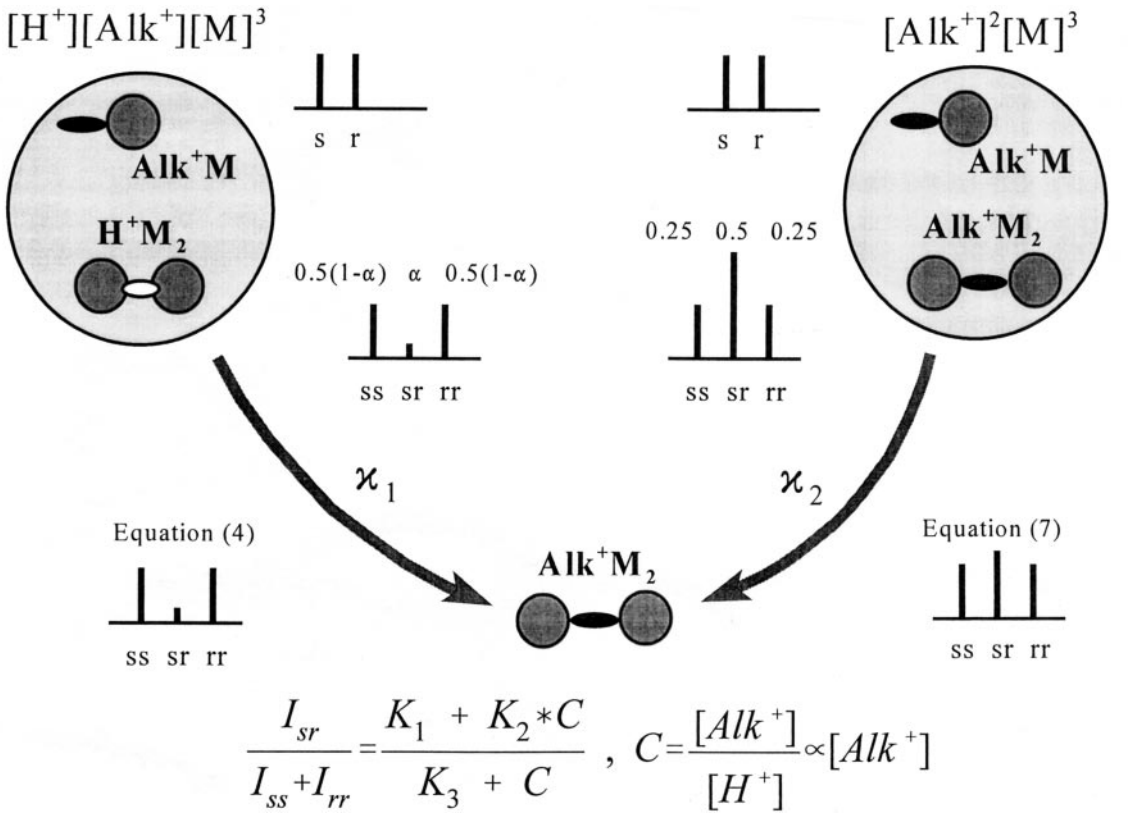

Fig. 7. Conceptual model of ESI microdroplets in final stage of dimer isolation with substitution of proton by alkali-ion adducts. Monomers and dimers are characterized by corresponding distributions. The two contributing channels form Table 1.

Let us now examine this simple model quantitatively. We assign "rate coefficients," k_1 and k_2 to the left-hand and right-hand droplet pathways, respectively, and summarize in Table 1 the parameters that are involved in the kinetics of alkali dimers.

The predicted chirality effect in the alkali-dimer group is expressed as follows:

$$\frac{I_{sr}}{I_{ss}+I_{rr}}=\frac{k_1\dfrac{4\beta(1+\alpha)}{6[(1-\alpha)+\beta(1+\alpha)]}[\mathrm{H}^+][\mathrm{Alk}^+]+k_2\dfrac{4\beta}{2+6\beta}[\mathrm{Alk}^+]^2}{k_1\dfrac{[6(1-\alpha)+2\beta(1+\alpha)]}{6[(1-\alpha)+\beta(1+\alpha)]}[\mathrm{H}^+][\mathrm{Alk}^+]+k_2\dfrac{2(1+\beta)}{2+6\beta}[\mathrm{Alk}^+]^2} \tag{8}$$

which leads to the simplified relationship

$$\frac{I_{sr}}{I_{ss}+I_{rr}}=\frac{K_1+K_2*C}{K_3+C}$$

where

$$C=[\mathrm{Alk}^+]/[\mathrm{H}^+] \tag{9}$$

$$K_2=\frac{2\beta}{1+\beta}$$

$$K_1=\frac{2k_1}{3k_2}\frac{\beta(1+3\beta)(1+\alpha)}{(1+\beta)[(1-\alpha)+\beta(1+\alpha)]}$$

$$K_3=\frac{2k_1(1+3\beta)[3(1-\alpha)+\beta(1+\alpha)]}{k_2\ (1+\beta)\ [6(1-\alpha)+\beta(1+\alpha)]}$$

Table 1
Droplet transient trimer kinetics model

Microdroplet components	"Rate"	Probability ~	Characteristic dimer distribution
(1) [H^+ dimer] + [Alk^+ + monomer]	k_1	[H^+]* [Alk^+]	See Eq. (4)
(2) [Alk^+ dimer] + [Alk^+ + monomer]	k_2	[Alk^+]^2	See Eq. (7)

The Fig. 6 experiment has been analyzed using this simplified model. Table 2 summarizes the results of the best fit to Eq. (9) for K_1, K_2, and K_3. For both Na^+ and Cs^+ K_2 is essentially unity, from which we conclude $\beta = 1$. This implies that the stability of the intermediate trimer in the liquid phase reaction intermediate is independent of their chirality. Having the β value defined enables us, in principle, to deduce both α and k_1/k_2 values from the best fit to Fig. 6. Experimental uncertainties in the Fig. 6 and Table 2 values for K_1 and K_3 do not provide a reliable value for α. Future experiments will provide more reliable values for α, k_1/k_2, and β and either verify or challenge our kinetic model.

Broadly speaking, there are two well-developed theories of microdroplet evolution in electrospray ionization which are supported by various experimental studies [9]. Iribarne and Thomson's model proposes that Coulomb instabilities lead to the evaporation of solvated ion clusters from the surface of droplets when their radii reach the order of 7–8 nm [10]. The competing mechanism, Dole's single ion in droplet (SID) model asserts that Rayleigh limit desolvation continues down to droplet sizes of the order of 1 nm diameter [11]. The present kinetics model of isolation of pairs of adducts in the final stage of solvent evaporation can be elaborated in the context of either model but fits more naturally into Dole's SID model. Specifically, ligand exchange at the last stage of desolvation is limited by the contents of microdroplets. Ligand concentrations are in turn proportional to the concentration and nature of species present in the bulk solution—e.g. protonated dimers and alkali ion tartrate monomers in the experiments reported here.

Table 2
Eq. (9) kinetics coefficients

	K_1	K_2	K_3
Na^+	$(2.0 \pm 0.7) \times 10^{-4}$	1.01 ± 0.03	$(3.2 \pm 1.0) \times 10^{-4}$
Cs^+	$(2.0 \pm 0.5) \times 10^{-5}$	1.00 ± 0.02	$(6.4 \pm 1.0) \times 10^{-5}$

3.3. Decomposition of gas phase trimers

A possible alternative explanation for these observations concerns the formation of metastable trimer cluster ions and the hypothesis that some fraction of the observed dimer distribution results from the dissociation of trimers in the gas phase. Electrosprayed alkali core ion trimers exhibit strong chirality effects, favoring homochiral structures. This special chirality effect in trimer ions is readily understood as resulting from the formation of "propeller" structures in which monomer ions of the same chiral configuration pack more closely around the core ion [2]. Obviously, if gas phase trimers decompose into protonated dimers during the approximate 0.5 s observation times of Fourier transform ion cyclotron resonance (FTICR) experiments, a pronounced apparent chirality effect would result.

The possible role of decomposition of gas phase trimers in determining the apparent chirality effect noted for alkali ion dimers cannot be entirely excluded, especially for higher concentrations of added salt and for higher concentrations of tartrates in solution. Indeed, preliminary experiments in which the trimer ion is a large fraction of total intensity evaluating the variation of the pseudochirality effect in Na^+ core ion dimers as a function of ion storage time in the hexapole storage region of the Analytica electrospray source indicate that significant decomposition of sodium dimethyl tartrate trimers occurs over the time scale of 0.05–0.5 s. However, decomposition of gas phase trimers shifts the distribution in the opposite direction than that given in Fig. 6. Additionally, only very low concentrations of trimers were

detected under our experimental conditions. For these reasons we do not consider this mechanism in our kinetics scheme for interpreting the low salt concentration and moderate tartrate concentration experiments with which we are primarily concerned in the present study.

4. Conclusions

In this research we have connected our earlier gas phase studies of molecular recognition in protonated and alkali ion core dimethyl tartrate dimers to a theoretical explanation for the equilibrium and kinetic effects investigated by FTMS methods. A satisfactory explanation is given for the observed chirality of the dimer cluster ions—namely the presence of hydrogen bonds in the protonated species and the essentially ionic bonding found for alkali ion core dimers. The intrinsic stability of these species predicted by theory is consistent with our experimental results for these species. The higher stability of ionically bound species rationalizes the displacement of the protonated species by alkali ion dimers (and trimers) when ligand exchange between the protonated and cation core clusters is possible.

When these experiments were extended to the liquid phase using electrospray ionization we found identical chirality effects for protonated species but quite different chirality for alkali ion core dimers. Because the properties of electrosprayed ions after isolation and examination in the ICR ion trap were identical to ions formed in the gas phase, we conclude that the apparent chirality effect is intimately connected to the mechanism of formation of microdroplets in the electrospray process in the final stages of their desolvation. A detailed kinetic model was developed which is consistent with our experimental findings and will be further tested in future research. This mictrodroplet model is generally consistent with general description of physical mechanisms of electrospray ionization.

The transient droplet trimer model developed in the paper provides the means to measure intrinsic chirality effects in aqueous solution even although the results precession was not sufficient to obtain the accurate values for α and k_1/k_2.

Acknowledgements

The support of this work by Civilian Research and Development Foundation grant no. RCI-204, by NSF grant no. CHE-9616711 and Russian Foundation for Basic Research, grant no. 96-03-32035a is gratefully acknowledged.

References

[1] M. Sawada, Mass Spectrom. Rev. 16 (1997) 73.
[2] E.N. Nikolaev, E.V. Denisov, V.S. Rakov, J.H. Futrell, F.J. Winkler, Adv. Mass Spectrom. 14 (1998) 279.
[3] H.M. Fales, G.J. Wright, J. Am. Chem. Soc. 99 (1977) 2339.
[4] E.V. Denisov, V. Shustryakov, E.N. Nikolaev, F.J. Winkler, R. Medina, Int. J. Mass Spectrom. Ion Processes 167/168 (1997) 259.
[5] E.N. Nikolaev, V.S. Rakov, J.H. Futrell, Presented at the 46th Annual Conference on Mass Spectrometry and Allied Topics, Orlando, FL, June 1998.
[6] GAUSSIAN 94, Revision D.4, M.J. Frisch, G.W. Trucks, H.B. Schlegel, P.M.W. Gill, B.G. Johnson, M.A. Robb, J.R. Cheeseman, T. Keith, G.A. Petersson, J.A. Montgomery, K. Raghavachari, M.A. Al-Laham, V.G. Zakrzewski, J.V. Ortiz, J.B. Foresman, J. Cioslowski, B.B. Stefanov, A. Nanayakkara, M. Challacombe, C.Y. Peng, P.Y. Ayala, W. Chen, M.W. Wong, J.L. Andres, E.S. Replogle, R. Gomperts, R.L. Martin, D.J. Fox, J.S. Binkley, D.J. Defrees, J. Baker, J.P. Stewart, M. Head-Gordon, C. Gonzalez, J.A. Pople, Gaussian, Inc., Pittsburgh, PA, 1995.
[7] A.D. Becke, J. Chem. Phys. 98 (1993) 5648.
[8] E.N. Nikolaev, T.B. McMahon, Presented at the 43th Annual Conference on Mass Spectrometry and Allied Topics, Atlanta, GA, May 21–26, 1995.
[9] P. Kebarle, L. Tang, Anal. Chem. 65 (1993) 972.
[10] J.V. Iribarne, B.A. Thomson, J. Chem. Phys. 64 (1976) 2287.
[11] M. Dole, L.L. Mack, R. Hines, R.C. Mobley, L.D. Ferguson, M.B. Alice, J. Chem. Phys. 49 (1968) 2240.